Temperature-Driven Switching of Helical Chirality of Poly[(4-carboxyphenyl)acetylene] Induced by a Single Amidine Enantiomer and Memory of the Diastereomeric Macromolecular Helicity

Takashi Hasegawa,[†,‡] Kazuhide Morino,[†] Yoshie Tanaka,[‡] Hiroshi Katagiri,[‡] Yoshio Furusho,[‡] and Eiji Yashima[*,†,‡]

Department of Molecular Design and Engineering, Graduate School of Engineering, Nagoya University, Chikusa-ku, Nagoya 464-8603, Japan, and Yashima Super-structured Helix Project, Exploratory Research for Advanced Technology (ERATO), Japan Science and Technology Agency (JST), 101 Creation Core Nagoya, 2266-22 Moriyama-ku, Nagoya 463-0003, Japan

Received October 11, 2005; Revised Manuscript Received November 14, 2005

ABSTRACT: Two novel optically active amidines, (*R*,*R*)-*N*,*N*′-bis(1-phenylethyl)-2,4,6-triphenylbenzamidine [(*R*,*R*)-**2**] and (*R*,*R*)-*N*,*N*′-bis(1-phenylethyl)benzamidine [(*R*,*R*)-**3**] were synthesized, and their helicity induction abilities for poly[(4-carboxyphenyl)acetylene] (poly-**1**) in dimethyl sulfoxide (DMSO) were investigated by UV−visible and circular dichroic spectroscopies. Poly-**1** exhibited a split-type induced circular dichroism (ICD) in the polymer backbone region in the presence of the optically active amidines due to a predominantly one-handed helical conformation. The ICD pattern of poly-**1** complexed with the bulky (*R*,*R*)-**2** ([(*R*,*R*)-**2**]/[poly-**1**] = 1) dramatically changed in DMSO and the Cotton effect signs reversibly inverted by changing the temperature, whereas the complex of poly-**1** with the less bulky (*R*,*R*)-**3** complex did not show such a temperature-driven change in the ICD. These results indicate that the helix-sense of poly-**1** induced by (*R*,*R*)-**2** through noncovalent acid−base interactions undergoes a transition from one helix to another in response to temperature. Furthermore, the diastereomeric right- and left-handed helices of poly-**1** induced by (*R*,*R*)-**2** at different temperatures could be separately memorized by the replacement of (*R*,*R*)-**2** with achiral amines, thus generating enantiomeric helices of the mirror images of each other.

Introduction

Amidines are strong organic bases that can effectively interact with carboxylic and phosphonic acids even in polar solvents.[1] This unique property of amidines has attracted significant attention, and a number of amidine-based receptors for the molecular recognition of synthetic and biologically active carboxylic and phosphonic acids[2] and molecularly imprinted gels[3] have been prepared. Chiral and achiral amidines have also been used as a key component for developing supramolecular liquid crystals,[4] chiral solids,[5] double helices,[6] and asymmetric catalysts.[7]

In a series of studies, we reported that the predominantly single-handed helix could be induced on a stereoregular, optically inactive poly(phenylacetylene) bearing a carboxy group (poly-**1**; Figure 1) upon complexation with optically active amines through noncovalent acid−base interactions.[8] The complexes exhibited a characteristic split-type induced circular dichroism (ICD) in the UV−visible region of the polymer backbone.[9] Furthermore, the right- or left-handed macromolecular helicity of poly-**1** induced by optically active amines could be "memorized" when the optically active amines were replaced by achiral amines such as 2-aminoethanol (**4**) and *n*-butylamine (**5**).[10] We recently reported the mechanism of helicity induction in poly-**1** with chiral amines and memory of the macromolecular helicity assisted by interaction with achiral amines, and the following important conclusions were drawn: (1) the ion pairing of poly-**1** with chiral amines is essential for the helicity induction, and (2) the electrostatic repulsion between the carboxylate groups of poly-**1** derived from the dissociation of the ion pairs plays a central role for the memory of helical chirality of poly-**1**.[10b]

In this study, we synthesized two novel optically active bulky and less bulky amidines, (*R*,*R*)-*N*,*N*′-bis(1-phenylethyl)-2,4,6-triphenylbenzamidine [(*R*,*R*)-**2**] and (*R*,*R*)-*N*,*N*′-bis(1-phenylethyl)benzamidine [(*R*,*R*)-**3**] (Figure 1), and their helicity induction abilities for poly-**1** were investigated in dimethyl sulfoxide (DMSO) by means of UV−visible and circular dichroism (CD) spectroscopies. We anticipated that the chiral amidines that may be more basic than the chiral primary amines might more effectively induce a one-handed helicity in poly-**1**. During the course of our study, we found that the helix-sense of poly-**1** induced by (*R*,*R*)-**2** at different temperatures could be switched by changing the temperature of the complex solution. Although several synthetic polymers bearing optically active substituents through covalent bonding[9,11] as well as biopolymers[12] are known to undergo a helix−helix transition by response to external chiral or achiral stimuli, inversion of a macromolecular helicity induced by optically active compounds through noncovalent bonding interactions responding to external stimuli is quite rare.[8d] Moreover, we also found that the resulting diastereomeric right- and left-handed helices of poly-**1** induced by (*R*,*R*)-**2** at different temperatures could be successfully memorized by the replacement of the amidine with achiral amines such as **4** and **5** (Figure 1). Accordingly, both mirror-image enantiomeric helices induced by a single enantiomer could be successfully produced from diastereomerically induced polyacetylenes assisted by the helicity inversion with temper-

* To whom correspondence should be addressed: e-mail yashima@apchem.nagoya-u.ac.jp.
† Nagoya University.
‡ ERATO, JST.

10.1021/ma052206w CCC: $33.50
Published on Web 12/23/2005

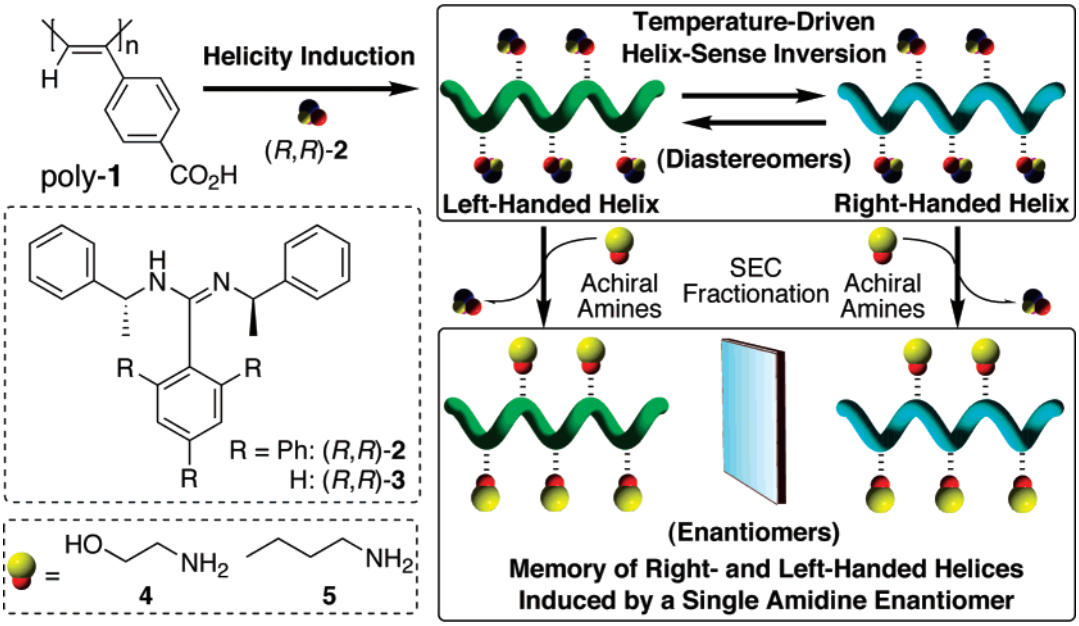

Figure 1. Schematic illustration of temperature-driven helix-sense inversion of the helical conformation of poly-**1** induced by an optically active amidine (*R*,*R*)-**2** and memory of the diastereomeric macromolecular helicity.

Scheme 1. Synthesis of Optically Active Amidines

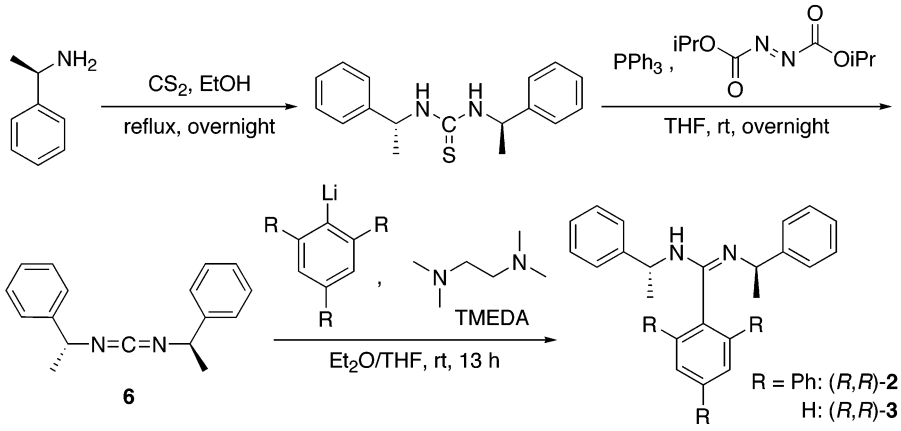

ature (Figure 1).[13] This helicity memory is different from the previous memory effect observed in poly-**1** in view of the fact that the opposite enantiomeric helicity memory requires the opposite enantiomeric amine, followed by the replacement with achiral amines.[10]

Experimental Section

Materials. Anhydrous tetrahydrofuran (THF, water content <0.005%) and ethanol (EtOH, water content <0.005%), *N*,*N*,*N*′,*N*′-tetramethylethylenediamine (TMEDA), and diisopropyl azodicarboxylate were purchased from Wako (Osaka, Japan). Anhydrous dimethyl sulfoxide (DMSO, water content <0.005%), *n*-butyllithium (1.6 M in *n*-hexane), and phenyllithium (1.9 M in cyclohexanes−ether) were obtained from Aldrich (Milwaukee, WI). Triphenylphosphine was available from Kishida (Osaka, Japan). (*R*)-1-Phenylethylamine was kindly supplied by Yamakawa Chemical (Tokyo, Japan), distilled under reduced pressure, and stored under nitrogen. 2-Aminoethanol (**4**) (Kishida) was dried over calcium oxide under nitrogen and distilled under reduced pressure. *n*-Butylamine (**5**) (Kishida) was dried over calcium hydride and distilled under nitrogen. These amines were stored under nitrogen.

Cis−transoidal poly-**1** was prepared by the polymerization of 4-ethynylbenzoic acid with $[Rh(nbd)_2]ClO_4$ (nbd = norbornadiene, Aldrich) in water in the presence of diethylamine at 30 °C for 3 h according to the previously reported method.[8c] The stereoregularity of the obtained polymer was investigated by measuring ^{1}H NMR and laser Raman spectroscopies and found to be almost completely cis−transoid.[14] The number-average molecular weight (M_n) and its distribution (M_w/M_n) of poly-**1** were estimated to be 13.0×10^4 and 4.3, respectively, as its methyl ester by size-exclusion chromatography (SEC) with polystyrene standards and chloroform as the eluent. Conversion of poly-**1** into the methyl ester was carried out by using diazomethane in diethyl ether according to the previously reported method.[8b] 2,4,6-Triphenylphenyl bromide[15] and 2,4,6-triphenylbenzoic acid[16] (**7**) were synthesized according to literature methods.

Synthesis of (*R*,*R*)-*N*,*N*′-Bis(1-phenylethyl)-2,4,6-triphenylbenzamidine ((*R*,*R*)-2). A novel optically active amidine (*R*,*R*)-2 was synthesized according to Scheme 1.

To a suspension of 2,4,6-triphenylphenyl bromide (380 mg, 1.00 mmol) in ether (2.0 mL) was added dropwise a 1.6 M *n*-hexane solution of *n*-butyllithium (0.65 mL, 1.05 mmol). The mixture was stirred at ambient temperature for 6 h. To the mixture was added dropwise TMEDA (115 mg, 1.0 mmol) and then a solution of carbodiimide **6** (200 mg, 0.8 mmol), which had been prepared according to the literature method,[17] in THF (2.0 mL). The resulting mixture was stirred at ambient temperature for 13 h. The mixture was then poured into water and extracted with ether (20 mL). The ethereal layer was washed with brine (10 mL) and then dried over anhydrous sodium sulfate. After filtration, the solvent was removed by evaporation. The residue was purified by column chromatog-

raphy [neutral alumina, hexane−ether = 9/1 (v/v)] to give 213 mg of (*R*,*R*)-**2** as a white solid in 48% yield based on **6** (mp 77.8−78.2 °C). IR (KBr, cm^{-1}): 3423 (N−H), 1637 (C═N). ^{1}H NMR (500 MHz, DMSO-d_6, 25 °C): δ 7.82−6.64 (m, 27H, aromatic protons), 6.53 (d, J = 5.7 Hz, 1H, NH), 4.88 (m, 1H, C*H*NH), 3.97 (q, J = 6.3 Hz, 1H, CHN═C), 1.30 (d, J = 6.8 Hz, 3H, *Me*CHNH), 0.38 (d, J = 6.0 Hz, 3H, *Me*CHN═C). ^{13}C NMR (125 MHz, DMSO-d_6, 25 °C): δ 152.11, 148.11, 146.00, 142.21, 141.34, 141.06, 140.07, 139.98, 139.24, 132.24, 129.15, 129.02, 128.81, 128.03, 127.85, 127.58, 127.49, 127.39, 127.35, 127.25, 126.93, 126.60, 126.15, 125. 97, 125.27, 125.10, 57.46, 49.24, 26.75, 22.18. Anal. Calcd for $C_{41}H_{36}N_2 \cdot {}^1/_5(H_2O)$: C, 87.88; H, 6.55; N, 5.00. Found: C, 87.84; H, 6.40; N, 4.91. $[\alpha]_D^{25}$ +25.3° (*c* 1.1, $CHCl_3$).

Synthesis of (*R*,*R*)-*N*,*N*′-Bis(1-phenylethyl)benzamidine [(*R*,*R*)-3].[18] This compound was prepared with **6** (1.9 g, 7.6 mmol) and phenyllithium in cyclohexane−ether (4.9 mL, 9.4 mmol) in the same way for the synthesis of (*R*,*R*)-**2** in 40% yield (505 mg) based on **6** as a slightly yellow solid (mp 121.3−121.4 °C). IR (KBr, cm^{-1}): 3406 (N−H), 1637 (C═N). ^{1}H NMR (500 MHz, DMSO-d_6, 25 °C): δ 7.39 (m, 5H, ArH), 7.30 (t, J = 7.6 Hz, 2H, ArH), 7.20 (t, J = 7.1 Hz, 1H, ArH), 7.10 (m, 2H, ArH), 6.96 (m, 3H, ArH), 6.76 (m, 2H, ArH), 6.61 (br d, J = 7.1 Hz, 1H, NH), 5.14 (m, 1H, C*H*NH), 4.02 (m, 1H, CHN═C), 1.38 (d, J = 6.8 Hz, 3H, *Me*CHNH). 1.16 (d, J = 6.3 Hz, 3H, *Me*CHN═C). Anal. Calcd for $C_{23}H_{24}N_2$: C, 84.11; H, 7.37; N, 8.53. Found: C, 84.26; H, 7.49; N, 8.46. $[\alpha]_D^{25}$ +40.8° (*c* 4.25, $CHCl_3$).

Instruments. The melting point was measured on a Yanako micro melting point apparatus and is uncorrected. NMR spectra were taken on a Varian VXR-500S spectrometer (500 MHz for ^{1}H and 125 MHz for ^{13}C) or Varian INOVA 700AS spectrometer (700 MHz for ^{1}H) in DMSO-d_6 with a solvent residual peak as the internal standard. Laser Raman spectra were measured on a Jasco NRS-1000 spectrophotometer. SEC was performed with a Jasco PU-980 liquid chromatograph equipped with a UV−visible detector (254 nm; Jasco UV-970) at 40 °C. A Tosoh TSKgel Multipore-H_{XL}-M SEC column was connected and chloroform was used as the eluent at a flow rate of 1.0 mL/min. The molecular weight calibration curve was obtained with polystyrene standards (Tosoh). IR spectra were recorded with a Jasco Fourier transform IR-620 spectrophotometer. The absorption and CD spectra were measured in a 0.1- or 4.0-mm quartz cell on a Jasco V-560 spectrophotometer and a Jasco J-725 spectropolarimeter, respectively, and the concentration of poly-**1** was calculated on the basis of the monomer units. Optical rotation was measured in a 5.0-cm quartz cell on a Jasco P-1030 polarimeter.

CD Measurements. A typical experimental procedure is described below. Stock solutions of poly-**1** (6 mg/mL, 41 mM) and (*R*,*R*)-**2** (41 mM) in DMSO were prepared. A 400 μL aliquot of the stock solution of poly-**1** was transferred to a vessel equipped with a screwcap by use of a Hamilton microsyringe. To the vessel was added 400 μL of the stock solution of (*R*,*R*)-**2** ([(*R*,*R*)-**2**]/[poly-**1**] = 1), and the initial CD and absorption spectra were measured in a 0.1-mm quartz cell immediately after the preparation of the solution. The sample solution was thermostated at 20 or 40 °C with a temperature-controlled water bath, and CD and absorption spectra were measured at appropriate time intervals at ambient temperature (24−26 °C).

Memory of Macromolecular Helicity: SEC Fractionation of Induced Helical Poly-1. Stock solutions of poly-**1** (6 mg/mL, 41 mM) and (*R*,*R*)-**2** (41 mM) in DMSO were prepared. A 800 μL aliquot of the stock solution of poly-**1** was transferred to a vessel equipped with a screwcap by use of a Hamilton microsyringe. To the vessel was added 800 μL of the stock solution of (*R*,*R*)-**2** ([(*R*,*R*)-**2**]/[poly-**1**] = 1). The solution was allowed to stand at 20 °C for 43 h, and then the CD and absorption spectra were measured at ambient temperature before SEC fractionation. SEC fractionation was performed on a Jasco PU-980 liquid chromatograph equipped with a UV (300 nm; Jasco UV-970) detector. A Shodex KF-806L SEC column (30 cm) was connected, and a DMSO solution of **4** (0.8 M) or **5** (0.008 M) was used as the mobile phase at a flow rate of 1.0 mL/min. An aliquot (100 μL) of the solution of poly-**1**−(*R*,*R*)-**2** complex ([poly-**1**] = 3 mg/mL, [(*R*,*R*)-**2**]/[poly-**1**] = 1) was injected to the SEC system, and the poly-**1** and (*R*,*R*)-**2** fractions were separately collected. The recovery of (*R*,*R*)-**2** was estimated on the basis of the UV spectrum of the (*R*,*R*)-**2** fraction with an ϵ value of (*R*,*R*)-**2** (ϵ_{275} = 19 970 M^{-1} cm^{-1}). The CD and absorption spectra of the fractionated poly-**1** were measured in a 4.0-mm quartz cell. The poly-**1**−(*R*,*R*)-**2** complex solution, which had been allowed to stand at 20 °C for 43 h, was then heated at 40 °C for 21 h and the CD and absorption spectra were measured at ambient temperature before SEC fractionation. The poly-**1** after inversion of the Cotton effect signs was isolated by SEC in the same way as that of the poly-**1** before inversion of the Cotton effect signs, and the CD and absorption spectra were measured.

X-ray Crystallographic Structure Determination. X-ray diffraction data for the complex of (*R*,*R*)-**2** with 2,4,6-triphenylbenzoic acid (**7**), a model compound of a bulky poly-**1**, were collected on a Bruker Smart Apex CCD-based X-ray diffractometer with Mo Kα radiation (λ = 0.710 73 Å) at 173 K.

Single crystals of **7**−(*R*,*R*)-**2** complex ($C_{72}H_{62}N_2O_3$, FW = 1003.24) suitable for X-ray analysis were grown by vapor diffusion of *n*-hexane into a benzene solution of **7**−(*R*,*R*)-**2** complex, and a single colorless crystal with dimensions of 0.50 × 0.40 × 0.20 mm was selected for intensity measurements (see Supporting Information).

Results and Discussion

Helicity Induction in Poly-1 with Chiral Amidines. Chiral amidines were prepared according to Scheme 1. 2,4,6-Triphenylphenyllithium obtained by the lithiation of 2,4,6-triphenylphenyl bromide with *n*-butyllithium and phenyllithium were allowed to react with (*R*,*R*)-*N*,*N*′-bis(1-phenylethyl)carbodiimide (**6**) to yield (*R*,*R*)-**2** and (*R*,*R*)-**3**, respectively. Poly-**1** (M_n = 13.0 × 10^4, M_w/M_n = 4.3) was prepared according to a previously reported method.[8c] Figure 2A (a and b) shows the typical CD spectra of poly-**1** in the presence of (*R*,*R*)-**2** and (*R*,*R*)-**3** in DMSO. The complexes ([**2** or **3**]/[poly-**1**] = 10) exhibited split-type intense ICDs in the polymer backbone region, and the ICDs were similar in pattern to those of the complexes of poly-**1** with other optically active primary amines in DMSO,[8−10] which indicates that poly-**1** can form a predominantly one-handed helix upon complexation not only with optically active amines but also with optically active amidines. The ICD intensities increased with increasing concentrations of (*R*,*R*)-**2** and (*R*,*R*)-**3**, but they did not reach a maximum value in the presence of 10 equiv of (*R*,*R*)-**2** and (*R*,*R*)-**3**; a further increase in the concentrations of the amidines caused precipitation of the complexes (Figure S-1 in Supporting Information).

The poly-**1**−(*R*,*R*)-**2** complexes exhibited ICDs with the negative second Cotton effects measured immediately after preparation of the samples independent of the amidine concentrations. However, interestingly, the poly-**1**−(*R*,*R*)-**2** complex ([(*R*,*R*)-**2**]/[poly-**1**] = 1) exhibiting a weak ICD with the negative second Cotton effect ($\Delta\epsilon_{second}$) (c in Figure 2A,B) slowly inverted from the negative to the positive direction at 20 °C, thus showing an intense positive second Cotton effect; after 43 h, the $\Delta\epsilon_{second}$ value reached an almost constant value (d in Figure 2A,B).[19] These ICD changes were accompanied by a slight blue shift of the absorption spectra (g and h in Figure 2A). The right- and left-handed helices of the poly-**1**−(*R*,*R*)-**2** complex induced by changing the temperature are not enantiomers but diastereomers due to the presence of the chiral amidine complexed with poly-**1**; therefore, their CD and absorption spectra differ from one another. Interestingly, the inverted Cotton effects reverted to almost the original ones upon heating the sample at 40 °C for 0.5 h (e in Figure 2A,B), and the intensity further increased in the negative direction at 40

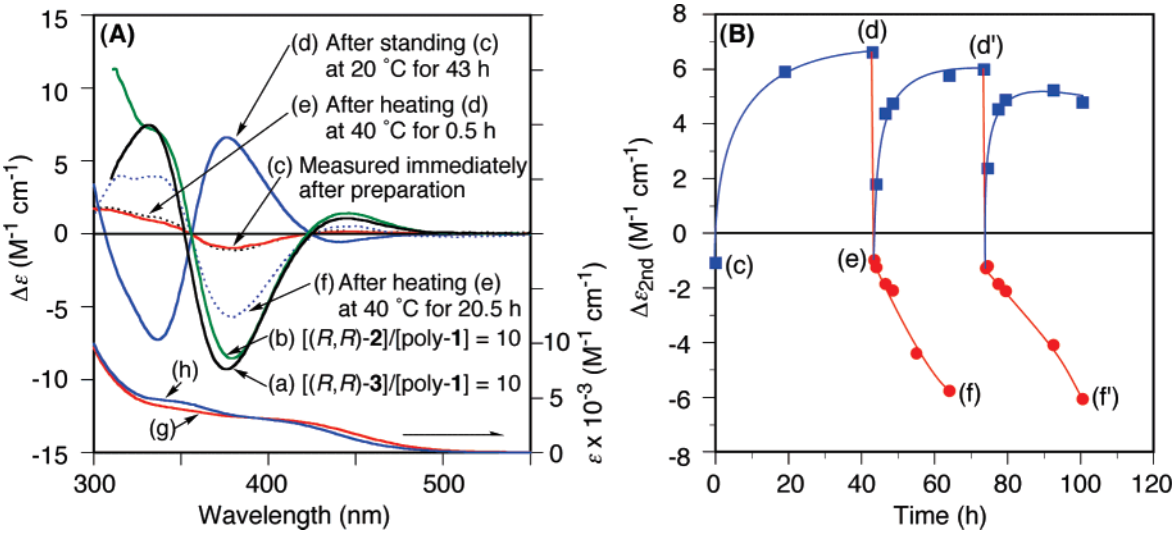

Figure 2. (A) CD spectra of poly-**1** (3 mg/mL) with (*R*,*R*)-**3** (a) and (*R*,*R*)-**2** (b) ([**2** or **3**]/[poly-**1**] = 10) and CD spectral changes of poly-**1**−(*R*,*R*)-**2** complex ([(*R*,*R*)-**2**]/[poly-**1**] = 1) (c−f) in DMSO. CD spectra of the poly-**1**−(*R*,*R*)-**2** complex were measured immediately after preparation of the sample (c), followed by allowing sample c to stand at 20 °C for 43 h (d), heating sample d at 40 °C for 0.5 h (e), and further heating sample e at 40 °C for 20.5 h (f). The CD spectra were measured at ambient temperature (24−26 °C). Absorption spectra of poly-**1** with (*R*,*R*)-**2** measured immediately after preparation of the sample and after standing at 20 °C for 43 h are also shown (g and h, respectively). (B) Changes in the $\Delta\epsilon_{second}$ values of the poly-**1**−(*R*,*R*)-**2** complex ([(*R*,*R*)-**2**]/[poly-**1**] = 1) in DMSO after the sample was allowed to stand at 20 °C (blue lines) and then heated at 40 °C (red lines); this cycle was repeated. The CD spectra at points c−f are shown in panel A.

°C with time (f in Figure 2A,B).[20] Although this change in the ICD was irreversible, when the solution of the poly-**1**−(*R*,*R*)-**2** complex (e in Figure 2A,B) was allowed to stand at 20 °C, the complex exhibited an intense ICD again with the positive second Cotton effect (d′ in Figure 2B). This cycle could be repeated (Figure 2B). These results demonstrate that the helix-sense of poly-**1** induced by (*R*,*R*)-**2** through noncovalent acid−base interactions can be reversibly controlled by changing the temperature.[21] On the other hand, such a helix-inversion phenomenon was not observed for the poly-**1**−(*R*,*R*)-**3** complex, indicating that the *m*-terphenyl moiety of (*R*,*R*)-**2** plays a role in the helix-inversion upon complexation with poly-**1**.

To gain insight into the mechanism of this unique helicity inversion of poly-**1** complexed with (*R*,*R*)-**2** with time, the change in its ^{1}H NMR spectrum was followed under the identical conditions as those for the CD measurements in Figure 2 (Figure 3). It is well-known that an *N*,*N*′-disubstituted amidine complexed with a carboxylic acid can exist in two configurational isomers; that is, the (*E*,*Z*) and (*E*,*E*) isomers (Figure 3B), which are in equilibrium depending on the solvent polarity, concentration, and temperature,[1] and the two isomers can be discriminated by ^{1}H NMR spectroscopy.[1b,c,6] In aprotic nonpolar solvents, the (*E*,*E*) isomer predominantly forms while the (*E*,*Z*) isomer prevails in protic and/or polar solvents.[1] In fact, the X-ray structural analysis of the crystal of (*R*,*R*)-**2** complexed with 2,4,6-triphenylbenzoic acid (**7**), a model compound of poly-**1**, obtained by vapor diffusion of *n*-hexane into a benzene solution of the complex, revealed that the amidinium group adopted the (*E*,*E*) configuration with the formation of the carboxylate−amidinium salt bridge through two hydrogen bonds with N···O distances of 2.66 and 2.80 Å (Figure 4). We assume that the two binding modes of the amidinium ion of (*R*,*R*)-**2** to the carboxylate ion of poly-**1** may play an important role in the time- and temperature-driven helix-sense inversion of poly-**1** in the polar solvent DMSO. The ^{1}H NMR spectrum of the poly-**1**−(*R*,*R*)-**2** complex ([poly-**1**] = 3 mg/mL, [(*R*,*R*)-**2**]/[poly-**1**] = 1) just after the sample preparation was similar in pattern to that of (*R*,*R*)-**2** and showed a pair of slightly broad resonances assigned to the nonequivalent methyl (ca. 0.4 and 1.3 ppm) and

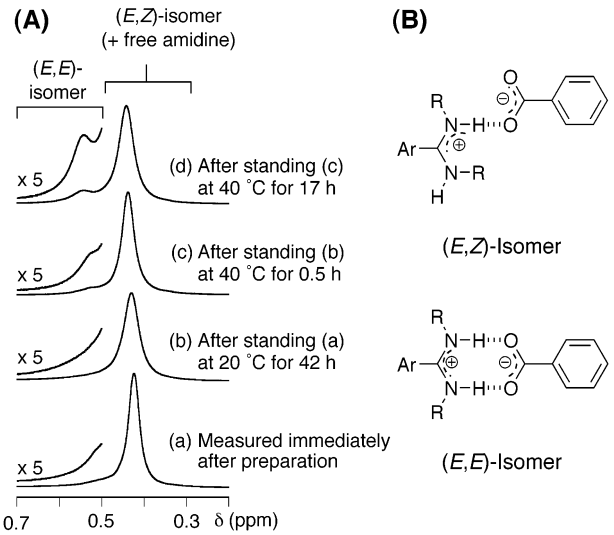

Figure 3. (A) 700 MHz ^{1}H NMR spectral changes of the complex of poly-**1** (3 mg/mL) with (*R*,*R*)-**2** ([(*R*,*R*)-**2**]/[poly-**1**] = 1) in DMSO-d_6. Shown are the ^{1}H NMR spectra of poly-**1**−(*R*,*R*)-**2** complex measured immediately after the sample preparation (a), followed by sample a allowed to stand at 20 °C for 42 h (b), sample b allowed to stand at 40 °C for 0.5 h (c), and sample c further allowed to stand at 40 °C for 17 h (d). The ^{1}H NMR spectra were measured at 25 °C under the identical conditions shown in Figure 2A; for the corresponding CD spectra for a−d, see c−f in Figure 2A, respectively. (B) Structures of (*E*,*E*) and (*E*,*Z*) isomers of benzoic acid *N*,*N*′-disubstituted amidine complex.

methine protons (ca. 4.0 and 4.9 ppm) for (*R*,*R*)-**2** (a and b in Figure S-2 in Supporting Information). Because the (*E*,*E*) isomer of (*R*,*R*)-**2** complexed with poly-**1** will show a set of single resonances due to the equivalent methyl and methine protons,[1,6] most of the (*R*,*R*)-**2** appeared to exist in the free form and a small portion as the (*E*,*Z*) form in the presence of poly-**1** in DMSO.[22] We note that a weak but apparent signal was observed at around 0.5−0.6 ppm (a in Figure 3A and b in Figure S-2) corresponding to the (*E*,*E*) isomer of (*R*,*R*)-**2** after the sample preparation.

To obtain further information, the ^{1}H NMR spectra of the complexes of the bulky **7** and less bulky vinylbenzoic acid

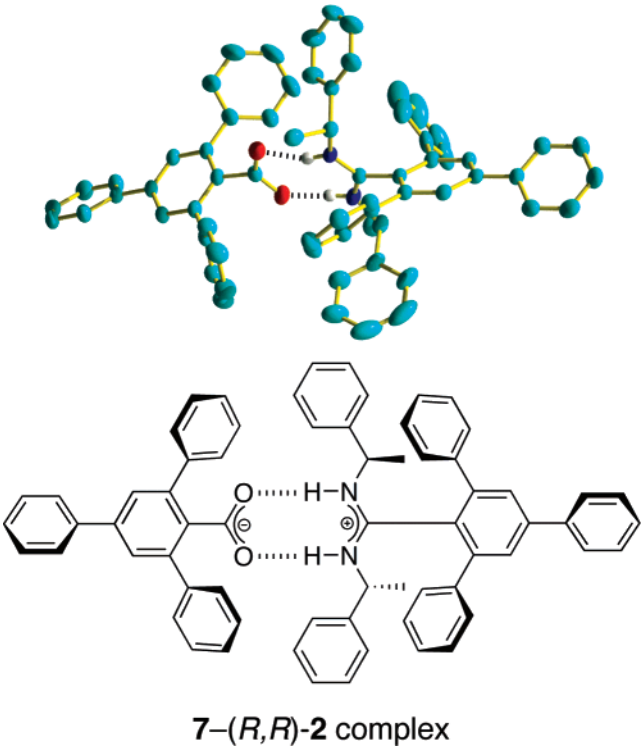

Figure 4. Crystal structure of **7**−(*R*,*R*)-**2** complex with thermal ellipsoids at 50% probability level. The hydrogen atoms except for those of the amidinium group and solvent molecules are omitted for clarity. The intermolecular hydrogen bonds between the amidine and carboxy groups are shown by dashed lines.

(VBA) with (*R*,*R*)-**2** were then measured in DMSO-d_6 or $CDCl_3$. The VBA− and **7**−(*R*,*R*)-**2** complexes showed a similar pair of resonances due to the nonequivalent methyl and methine protons of (*R*,*R*)-**2** as well as the minor and equivalent resonances at 0.60 and 4.14 ppm and at 0.38 and 3.97 ppm in DMSO-d_6, respectively (c and d in Figure S-2). The latter peaks can be assigned to those of the (*E*,*E*) isomer,[6] because the peak intensities increased with the increasing volume fraction of $CDCl_3$ in DMSO-d_6 accompanied by a decrease in the intensities of the peaks derived from the free **2** and (*E*,*Z*)-**2** methyl and methine protons; in pure $CDCl_3$, the (*E*,*E*) form is predominant and the (*R*,*R*)-**2** complex with **7** exhibited two single peaks in the methyl (0.50 ppm) and methine (3.89 ppm) proton resonance regions (e in Figure S-2).[1,6] These results indicate that the weak signal at around 0.5−0.6 ppm observed for the poly-**1**−(*R*,*R*)-**2** complex ([poly-**1**] = 3 mg/mL, [(*R*,*R*)-**2**]/[poly-**1**] = 1) just after the sample preparation could be assigned to the methyl protons of the (*E*,*E*) isomer (a in Figure 3A and b in Figure S-2). Interestingly, however, this signal seems to disappear after storage of the sample at 20 °C for 42 h accompanied by the broadening of the peak at 0.42 ppm (b in Figure 3A). Upon heating the sample at 40 °C for 0.5 h, a rather sharp signal due to the (*E*,*E*) isomer appeared in the region, whose intensity further increased with time (c and d in Figure 3A). This increase in the peak intensity was accompanied by a decrease in the peak intensity at 0.42 ppm corresponding to the free and (*E*,*Z*) forms of (*R*,*R*)-**2**. These changes in the ^{1}H NMR spectra reversibly occurred as well as those in the CD inversion (Figure 2B). On the basis of these observations, we presumed that the temperature-driven helix-sense inversion of the poly-**1**−(*R*,*R*)-**2** complex in DMSO may be ascribed to the isomerization between the (*E*,*Z*) and (*E*,*E*) isomers of (*R*,*R*)-**2** upon complexation with poly-**1** (Figure 5).[23] Apparently, further experiments including

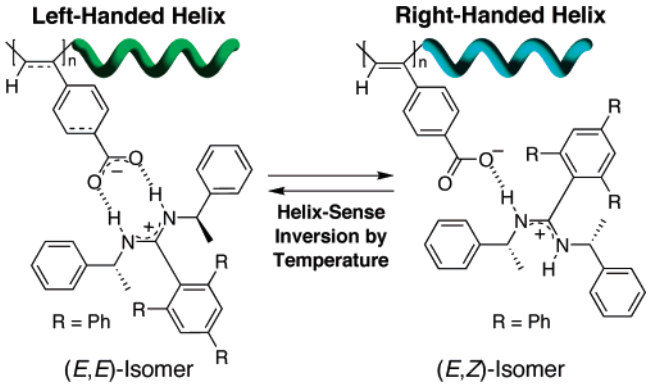

Figure 5. Schematic illustration of the mechanism of helix-sense inversion of the helical conformation of poly-**1** induced by (*R*,*R*)-**2**. The helix-senses of poly-**1** are tentatively assigned on the basis of the Cotton effect signs of the ICDs of poly-**1** complexed with optically active amines.[8d]

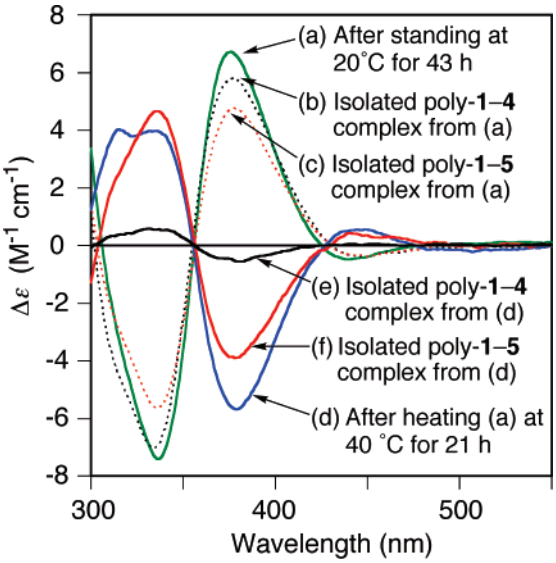

Figure 6. CD spectra of poly-**1**−(*R*,*R*)-**2** complex ([poly-**1**] = 3 mg/mL, [(*R*,*R*)-**2**]/[poly-**1**] = 1), after standing at 20 °C for 43 h (a) and then after sample a was heated at 40 °C for 21 h (d), and the isolated poly-**1**s by SEC fractionation with a DMSO solution of **4** (0.8 M) (b, e) or **5** (0.008 M) (c, f) as the mobile phase, in DMSO at ambient temperature (24−26 °C).

the solvent effects on the helicity induction of poly-**1** with (*R*,*R*)-**2** and the (*E*,*Z*)−(*E*,*E*) isomerization are necessary.

Memory of the Diastereomeric Macromolecular Helicities of Poly-1. We then investigated whether the diastereomeric right- and left-handed helices of poly-**1** induced by (*R*,*R*)-**2** could be memorized by replacing (*R*,*R*)-**2** with achiral amines such as **4** and **5**. The poly-**1**−(*R*,*R*)-**2** complex showing a positive $\Delta\epsilon_{second}$ value (+6.71) (a in Figure 6 and d in Figure 2A) was initially used for the memory experiments, and the memorized poly-**1** was isolated from the complex solution by SEC with a DMSO solution of **4** (0.8 M) or **5** (0.008 M) as the eluent. These achiral amines were selected because they were good chaperoning molecules to assist in the memory of the macromolecular helicity of poly-**1** induced by the optically active primary amines in DMSO.[10] The isolated poly-**1** complexed with achiral **4** or **5** exhibited an intense ICD despite the complete removal of the (*R*,*R*)-**2** by SEC (b and c in Figure 6, respectively).[24] These results indicate that the helical chirality of poly-**1** induced by (*R*,*R*)-**2** can also be memorized by the replacement of (*R*,*R*)-**2** with achiral amines. The memory efficiencies estimated from the ICD value of the poly-**1**−(*R*,*R*)-**2** complex before the SEC

Table 1. Memory Efficiencies of the Macromolecular Helicity of Poly-1 Induced by (*R*,*R*)-2 with Achiral Amines (4 and 5)

helical poly-**1** in Figure 2B[a] [$\Delta\epsilon_{second}$ (M^{-1} cm^{-1}) (λ (nm))]	achiral amine[b] (M)	isolated poly-**1**	
		$\Delta\epsilon_{second}$ (M^{-1} cm^{-1}) (λ (nm))	memory efficiency[c] (%)
(d) [+6.71 (376)]	**4** (0.8)	+5.82 (377)	86[d]
(d) [+6.71 (376)]	**4** (0.08)	+3.68 (377)	55
(d) [+6.71 (376)]	**4** (0.008)	+2.32 (377)	35
(d) [+6.71 (376)]	**5** (0.8)	+4.54 (377)	68
(d) [+6.71 (376)]	**5** (0.08)	+4.41 (377)	66
(d) [+6.71 (376)]	**5** (0.008)	+4.77 (377)	71[e]
(f) [−5.75 (379)]	**4** (0.8)	−0.55 (381)	10[f]
(f) [−5.75 (379)]	**5** (0.008)	−3.89 (378)	68[g]
(d′) [+5.98 (376)]	**4** (0.8)	+4.90 (376)	82
(d′) [+5.98 (376)]	**5** (0.008)	+3.99 (376)	67
(f′) [−6.06 (379)]	**4** (0.8)	−0.48 (380)	8
(f′) [−6.06 (379)]	**5** (0.008)	−3.99 (378)	66

[a] Helical poly-**1**s induced by (*R*,*R*)-**2** were memorized at those points in Figure 2B (see d−f′). [b] Concentrations of achiral amines in DMSO as the mobile phase for the SEC fractionation are shown in parentheses. [c] Memory efficiencies (%) were estimated on the basis of the ICD values at $\Delta\epsilon_{second}$ just after the SEC fractionation of the poly-**1**−(*R*,*R*)-**2** complex solution ([poly-**1**] = 3 mg/mL, [(*R*,*R*)-**2**]/[poly-**1**] = 1) with achiral amines in DMSO as the mobile phase. [d] See Figure 6b. [e] See Figure 6c. [f] See Figure 6e. [g] See Figure 6f.

fractionations as the base value were 86% and 71% for **4** and **5**, respectively (Table 1).[25] In the same way, the diastereomeric, opposite helical poly-**1**−(*R*,*R*)-**2** complex with a negative second Cotton effect obtained at 40 °C (d in Figure 6 and f in Figure 2) was also successfully memorized (e and f in Figure 6). Although the memory efficiency with **4** was rather low (ca. 10%), the helical chirality could be memorized with a 68% memory efficiency for **5** (Table 1). The ICD patterns of the memorized poly-**1**s obtained from the two diastereomeric helices of the poly-**1**−(*R*,*R*)-**2** complex with the opposite Cotton effect signs from each other were complete mirror images, indicating that the separated species correspond to enantiomeric right- and left-handed helices (Figure 6).[26] The isolated poly-**1**s maintained the helicity memory for over 6 months at ambient temperature. In the same manner, the diastereomeric helices of the poly-**1**−(*R*,*R*)-**2** complex obtained from the second helix-inversion process (d′ and f′ in Figure 2B) could also be memorized (Table 1).

Conclusions

In summary, we have found that the macromolecular helicity of poly-**1** can be induced by optically active amidines through noncovalent acid−base interactions, and poly-**1** complexed with a bulky chiral amidine undergoes a helix−helix transition from one helix to another in response to temperature. The resulting diastereomeric helices obtained at different temperatures induced by a single enantiomeric amidine could be further memorized by replacement of the amidine with achiral amines, thus generating both mirror-image enantiomeric helices. We expect that a similar dual memory of enantiomeric helices induced by a single enantiomer will be possible in other switchable, dynamic helical polyacetylenes bearing rationally designed functional pendants.

Acknowledgment. This work was partially supported by a Grant-in-Aid for Scientific Research from Japan Society for the Promotion of Science and the 21st Century COE Program "Nature-Guided Materials Processing" of the Ministry of Education, Culture, Sports, Science, and Technology, Japan.

Supporting Information Available: Figures showing the titration curves of the ICD intensity ($\Delta\epsilon_{second}$) in the complexation of poly-**1** ([poly-**1**] = 3 mg/mL) with (*R*,*R*)-**2** and (*R*,*R*)-**3** in DMSO, ^{1}H NMR spectra of (*R*,*R*)-**2** and poly-**1**− and VBA−(*R*,*R*)-**2** complexes in DMSO-d_6, and **7**−(*R*,*R*)-**2** complex in DMSO-d_6 and $CDCl_3$; text giving experimental information on the X-ray structural information, including a figure showing an ORTEP diagram and a table of crystallographic data (PDF); and an X-ray crystallographic file (CIF). This material is available free of charge via the Internet at http://pubs.acs.org.

References and Notes

(1) (a) Papoutsakis, D.; Kirby, J. P.; Jackson, J. E.; Nocera, D. G. *Chem.—Eur. J.* **1999**, *5*, 1474−1480. (b) Peters, L.; Fröhlich, R.; Boyd, A. S. F.; Kraft, A. *J. Org. Chem.* **2001**, *66*, 3291−3298. (c) Kraft, A.; Peters, L.; Powell, H. R. *Tetrahedron* **2002**, *58*, 3499−3505. (d) Otsuki, J.; Iwasaki, K.; Nakano, Y.; Itou, M.; Araki, Y.; Ito, O. *Chem.—Eur. J.* **2004**, *10*, 3461−3466. (e) Damrauer, N. H.; Hodkiss, J. M.; Rosenthal, J.; Nocera, D. G. *J. Phys. Chem. B* **2004**, *108*, 6315−6321.

(2) (a) Göbel, M. W.; Bats, J. W.; Dürner, G. *Angew. Chem., Int. Ed. Engl.* **1992**, *31*, 207−209. (b) Grawa, T.; Schrader, T.; Gurrath, M.; Kraft, A.; Osterod, F. *Org. Lett.* **2000**, *2*, 29−32. (c) Grawa, T.; Schrader, T.; Zadmard, R.; Kraft, A. *J. Org. Chem.* **2002**, *67*, 3755−3763. (d) Corbellini, F.; Costanzo, L. D.; Crego-Calama, M.; Geremia, S.; Reinhoutd, D. N. *J. Am. Chem. Soc.* **2003**, *125*, 9946−9947.

(3) (a) Wulff, G.; Schönfeld, R. *Adv. Mater.* **1998**, *10*, 957−959. (b) Embenbroich, M.; Wulff, G. *Chem.—Eur. J.* **2003**, *9*, 4106−4117. (c) Liu, J.; Wulff, G. *Angew. Chem., Int. Ed.* **2004**, *43*, 1287−1290.

(4) Kraft, A.; Reichert, A. *Tetrahedron* **1999**, *55*, 3923−3930.

(5) Hosseini, M. W. *Coord. Chem. Rev.* **2003**, *240*, 157−166.

(6) Tanaka, Y.; Katagiri, H.; Furusho, Y.; Yashima, E. *Angew. Chem., Int. Ed.* **2005**, *44*, 3867−3870.

(7) (a) Saitoh, A.; Achiwa, K.; Tanaka, K.; Morimoto, T. *J. Org. Chem.* **2000**, *65*, 4227−4240. (b) Hu, X.; Chen, H.; Dai, H.; Hu, X.; Zheng, Z. *Tetrahedron: Asymmetry* **2003**, *14*, 2073−2080.

(8) (a) Yashima, E.; Matsushima, T.; Okamoto, Y. *J. Am. Chem. Soc.* **1995**, *117*, 11596−11597. (b) Yashima, E.; Matsushima, T.; Okamoto, Y. *J. Am. Chem. Soc.* **1997**, *119*, 6345−6359. (c) Saito, M. A.; Maeda, K.; Onouchi, H.; Yashima, E. *Macromolecules* **2000**, *33*, 4616−4618. (d) Maeda, K.; Morino, K.; Yashima, E. *J. Polym. Sci., Part A: Polym. Chem.* **2003**, *41*, 3625−3631. (e) Onouchi, H.; Hasegawa, T.; Kashiwagi, D.; Ishiguro, H.; Maeda, K.; Yashima, E. *Macromolecules* **2005**, *38*, 8625−8633.

(9) (a) Yashima, E. *Anal. Sci.* **2002**, *18*, 3−6. (b) Yashima, E.; Maeda, K.; Nishimura, T. *Chem.—Eur. J.* **2004**, *10*, 42−51.

(10) (a) Yashima, E.; Maeda, K.; Okamoto, Y. *Nature* **1999**, *399*, 449−451. (b) Maeda, K.; Morino, K.; Okamoto, Y.; Sato, T.; Yashima, E. *J. Am. Chem. Soc.* **2004**, *126*, 4329−4342. (c) Morino, K.; Watase, N.; Maeda, K.; Yashima, E. *Chem.—Eur. J.* **2004**, *10*, 4703−4707.

(11) For recent reviews, see (a) Green, M. M.; Cheon, K.-S.; Yang, S.-Y.; Park. J.-W.; Swansburg, S.; Liu, W. *Acc. Chem. Res.* **2001**, *34*, 672−680. (b) Cornelissen. J. J. L. M.; Rowan, A. E.; Nolte, R. J. M.; Sommerdijk, N. A. J. M. *Chem. Rev.* **2001**, *101*, 4039−4070. (c) Nakano, T.; Okamoto, Y. *Chem. Rev.* **2001**, *101*, 4013−4038. (d) Fujiki, M. *Macromol. Rapid. Commun.* **2001**, *22*, 539−563. (e) Fujiki, M.; Koe, J. R.; Terao, K.; Sato, T.; Teramoto, A.; Watanabe, J. *Polym. J.* **2003**, *35*, 297−344. (f) Lam, J. W. Y.; Tang, B. Z. *Acc. Chem. Res.* **2005**, *38*, 745−754. For leading references, see (g) Yashima, E.; Maeda, Y.; Okamoto, Y. *J. Am. Chem. Soc.* **1998**, *120*, 8895−8896. (h) Fujiki, M. *J. Am. Chem. Soc.* **2000**, *122*, 3336−3343. (i) Cheon, K. S.; Selinger, J. V.; Green, M. M. *Angew. Chem., Int. Ed.* **2000**, *39*, 1482−1485. (j) Yashima, E.; Maeda, K.; Sato, O. *J. Am. Chem. Soc.* **2001**, *123*, 8159−8160. (k) Nakako, H.; Nomura, R.; Masuda, T. *Macromolecules* **2001**, *34*, 1496−1502. (l) Tang, K.; Green, M. M.; Cheon, K. S.; Selinger, J. V.; Garetz, B. A. *J. Am. Chem. Soc.* **2003**,

125, 7313−7323. (m) Morino, K.; Maeda, K.; Yashima, E. *Macromolecules* **2003**, *36*, 1480−1486. (n) Cheuk, K. K. L.; Lam, J. W. Y.; Chen, J.; Lai, L. M.; Tang, B. Z. *Macromolecules* **2003**, *36*, 5947−5959. (o) Cheuk, K. K. L.; Lam, J. W. Y.; Lai, L. M.; Dong, Y.; Tang, B. Z. *Macromolecules* **2003**, *36*, 9752−9762. (p) Maeda, K.; Kamiya, N.; Yashima, E. *Chem.—Eur. J.* **2004**, *10*, 4000−4010. (q) Ohira, H.; Kunitake, M.; Fujiki, M.; Naito, M.; Saxena, A. *Chem. Mater.* **2004**, *16*, 3919−3923. (r) Zhao, H.; Sanda, F.; Masuda, T. *Macromol. Chem. Phys.* **2005**, *206*, 1653−1658. (s) Tang, H. Z.; Boyle, P. D.; Novak, B. M. *J. Am. Chem. Soc.* **2005**, *127*, 2136−2142.

(12) (a) Pohl, F. M.; Jovin, T. M. *J. Mol. Biol.* **1972**, *67*, 375−396. (b) Toriumi, H.; Saso, N.; Yasumoto, Y.; Sasaki, S.; Uematsu, I. *Polym. J.* **1979**, *11*, 977−981. (c) Watanabe, J.; Okamoto, K.; Satoh, K.; Sakajiri, K.; Furuya, H. *Macromolecules* **1996**, *29*, 7084−7088. (d) Tashiro, R.; Sugiyama, H. *J. Am. Chem. Soc.* **2005**, *127*, 2094−2097.

(13) Recently, we have found that both enantiomeric helices can be produced from dynamically diastereomeric helices of a poly(phenylacetylene) bearing a bulky phenyl phosphonate group at the pendant induced by a single enantiomeric primary amine based on the noncovalent "helicity induction and chiral memory" concept assisted by temperature-stimulated helix-inversion of the polymer. Miyagawa, T.; Furuko, A.; Maeda, K.; Katagiri, H.; Furusho, Y.; Yashima, E. *J. Am. Chem. Soc.* **2005**, *127*, 5018−5019.

(14) (a) Simionescu, C. I.; Percec, V.; Dumitrescu, S. *J. Polym. Sci: Polym. Chem. Ed.* **1977**, *15*, 2497−2509. (b) Simionescu, C. I.; Percec, V. *Prog. Polym. Sci.* **1982**, *8*, 133-214. (c) Furlani, A.; Napoletano, C.; Russo, M. V.; Feast, W. J. *Polym. Bull.* **1986**, *16*, 311−317. (d) Matsunami, S.; Kakuchi, T.; Ishii, F. *Macromolecules* **1997**, *30*, 1074−1078. (e) Kishimoto, Y.; Eckerle, P.; Miyatake, T.; Kainosho, M.; Ono, A.; Ikariya, T.; Noyori, R. *J. Am. Chem. Soc.* **1999**, *121*, 12035−12044. (f) Percec, V.; Rudick, J. G. *Macromolecules* **2005**, *38*, 7241−7250.

(15) Haaland, A.; Rypdal, K.; Hans, P.; Scherer, W.; Thiel, W. R. *Angew. Chem., Int. Ed. Engl.* **1994**, *33*, 2443−2445.

(16) Barclay, L. R. C.; Sonawane, H. R.; Hudson, J. C. *Can. J. Chem.* **1972**, *50*, 2318−2325.

(17) Chinchilla, R.; Nájera, C.; Sánchez-Agulló, P. *Tetrahedron: Asymmetry* **1994**, *5*, 1393−1402

(18) (a) Brunner, H.; Lukassek, J.; Agrifoglio, G. *J. Organomet. Chem.* **1980**, *195*, 63−76. (b) Korp, J. D.; Bernal, I. *Chem. Scr.* **1983**, *22*, 60−63.

(19) The changes in the Cotton effect sign of the poly-**1**−(*R*,*R*)-**2** complex were highly dependent on the molar ratio ([(*R*,*R*)-**2**]/[poly-**1**]) and temperature and were hardly observed when [(*R*,*R*)-**2**]/[poly-**1**] ≥ 3. At 25 °C, the ICD changes more rapidly occurred at [(*R*,*R*)-**2**]/[poly-**1**] = 2, but the complex precipitated after 32 h. Therefore, we employed the poly-**1**−(*R*,*R*)-**2** complex ([(*R*,*R*)-**2**]/[poly-**1**] = 1) for the CD inversion experiments.

(20) Further ICD changes could not be followed because of precipitation of the poly-**1**−(*R*,*R*)-**2** complex at 40 °C.

(21) The poly-**1**−(*R*,*R*)-**2** complex prepared under nitrogen and then stored in a sealed ampule also showed the identical temperature-driven helix-sense inversion, indicating that the effect of water on the helix-sense inversion could be ruled out.

(22) The binding constant (*K*) of (*R*,*R*)-**2** with poly-**1** (3 mg/mL), estimated by IR titration experiments according to the previously reported method,[10b] was 20 M^{-1} in DMSO, indicating that the bulky amidine cannot interact with poly-**1** as strongly as the primary amines in DMSO.[10b] On the basis of the *K* value, ca. 25% of (*R*,*R*)-**2** interacts with poly-**1** under the conditions of ^{1}H NMR and CD measurements ([(*R*,*R*)-**2**]/[poly-**1**] = 1).

(23) The mechanism of the time- and temperature-dependent isomerization between the (*E*,*Z*) and (*E*,*E*) isomers of the poly-**1**−(*R*,*R*)-**2** complex is not clear at present, but a bulky *m*-terphenyl group of (*R*,*R*)-**2** complexed with poly-**1** may play an important role in the isomerization, resulting in the inversion of the poly-**1** helicity, because the CD and ^{1}H NMR spectra of the poly-**1**−(*R*,*R*)-**3** complex and the ^{1}H NMR spectrum of the **7**−(*R*,*R*)-**2** complex did not exhibit such time- and temperature-dependent changes.

(24) On the basis of the UV spectra of the (*R*,*R*)-**2** fractions collected during the memory experiments by SEC, more than 99% of the (*R*,*R*)-**2** was recovered.

(25) The memory efficiency decreased with decreasing concentration of **4** in the mobile phase, whereas we found no significant changes in the memory efficiency in the concentration ranges of 0.8−0.008 M for **5** (Table 1). Therefore, we set the concentrations of **4** and **5** in the mobile phase at 0.8 and 0.008 M, respectively.

(26) The macromolecular helicities of poly-**1** induced by 10 equiv of (*R*,*R*)-**2** and (*R*,*R*)-**3** ($\Delta\epsilon_{2nd}$ = −8.55 and −9.30, respectively) could also be memorized with **4** and **5**; the respective memory efficiencies were 75% and 93% for **4** and 86% and 86% for **5**.

MA052206W